Combined strategy for control of interaction force between manipulator and flexible environment

Piotr Gierlak

Faculty of Mechanical Engineering and Aeronautics, Department of Applied Mechanics and Robotics, Rzeszow University of Technology, 35-959, Rzeszów, Poland, (e-mail: pgierlak@prz.edu.pl)

Abstract: The article discusses the question of a combined strategy for control of interaction force between a manipulator and a flexible environment, aimed at conducting robotized machining of surfaces of disturbed shape, taking into account their flexibility. The control strategy combines, on the basis of competitiveness, two elementary control strategies. The first one aims at conducting the desired interaction force, whereas the objective of the latter is to model the nominal shape of the processed surface. In the event the shape of the real surface differs from the nominal shape, the actions of both strategies become competitive. A combination of two strategies which allows selecting a middle solution automatically and which allows each strategy to be executed in a „soft" way has been set forth.

Keywords: Force control, robotic manipulators, control algorithms, nonlinear control, constraints.

1. INTRODUCTION

Manipulators are becoming more and more frequently applied in the broadly defined industry, which requires the realization of a desired motion path of the manipulator end-effector with simultaneous control of the forces of interaction with the environment. Currently, attempts are being made to provide a precise control of forces in order to ensure proper execution of processes such as grinding, chamfering, polishing, etc. (Lotz et al.,2014; Tian et al., 2016; Yu et al., 2011). The problem of contact between the manipulator and the environment is associated with partial restrictions of the manipulator's motion, i.e. the existence of constraints.

In the field of robotized machining, the environment with which a robot interacts is understood as a surface or an edge which is contacted by the robot by means of an end-effector. The end-effector is equipped with a tool for a specific task. A crucial and still relevant issue connected with robotized machining is designing and implementing control strategies which ensure appropriate machining quality despite the occurrence of non-modeled events, such as significant errors in the environment description arising out of the uncertainty of its location with regards to the robot or local distortions of the environment surface (Fanaei and Farrokhi, 2006; Ferguene and Toumi, 2009; Liu et al., 2007; Pliego-Jiménez and Arteaga-Pérez, 2015).

Nowadays, in the field of industrial robotics, two elementary strategies of force control prevail (Application manual, 2011). The first one is based on maintaining a constant interaction force together with a constant motion velocity, and the trajectory is automatically adjusted to the shape of the contact surface (Fig. 1a). Disadvantages of such a solution become noticeable in the following case: If the surface is processed with the use of a tool of a small contact surface and there is e.g. a cavity in the surface, the cavity will be deepened with each passage of the tool, which is a result of exercising constant clamping force and automatic adjustment of the trajectory to the surface profile. Nonetheless, this method is very effective in processes such as e.g. polishing, when the processed surface is devoid of significant cavities and the tool has a large operative surface. The second control strategy is based on the motion of the manipulator end-effector along the desired trajectory, regardless of the shape of the processed surface (Fig. 1b). In this case, the variable value is motion velocity, which is dependable on motion resistance. In case there is some excess material on the processed surface, significant motion resistance occurs and the motion velocity decreases. In the case of this strategy, clamping force is not a controlled value, but is dependent on the desired trajectory and the actual shape of the contact surface. This strategy is similar to CNC machining methods, but the difference is based on the fact that the slide velocity depends on tangential forces. The disadvantage of this method is a risk of loss of contact between the manipulator end-effector and the surface if the desired trajectory

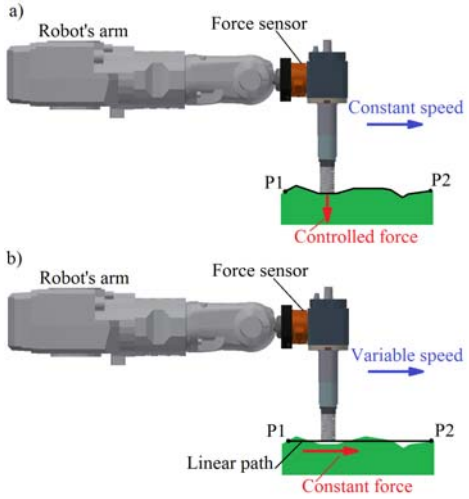

Fig. 1. Main strategies for force control applied in industry.

significantly diverges from the actual location of the contact surface, or otherwise, it may lead to excessive drilling of the manipulator end-effector into the material. The names of the aforesaid strategies may differ in commercial applications, yet the subject-matter remains the same. Sometimes the basic control strategies are modified in order to introduce certain adjustability into the way they are executed; nonetheless, they are still two separate strategies.

Successful implementation of the selected control strategies is strictly connected with capabilities and methods of measurement of interaction forces between the manipulator and its environment. In the writings on manipulator force control, one can find basically three approaches which are used to measure these forces. In one of these approaches, the interaction force is defined as a product of the assumed stiffness and the deformation of the environment, whereas the deformation of the environment is determined by means of measurement of the location of the manipulator end-effector (Wu and Chen, 2011). Determining deformation requires a precise knowledge of the actual environment surface location and the knowledge of the current location of the manipulator end-effector. The application of such an approach requires the calibration of kinematic parameters of the manipulator. Otherwise, this method fails to give appropriate results. A different approach is the application of a method based on a direct measurement of forces by means of a force sensor in the manipulator end-effector (Xiao et al., 2000). Such a force measurement does not require adopting an environment model, which like every model is flawed by errors and modeling uncertainty. It does not require assuming the stiffness of the environment. During the motion of the manipulator with accelerations, a disadvantage of this approach is revealed, that is, the measurement of forces is distorted by the components of fictitious forces. Nevertheless, these distortions are not significant, as the accelerations in the tasks in which the interaction between manipulator and its environment occurs are low. There is also a middle solution based on measurement of forces in the manipulator joints and determining forces in its end-effector with the use of kinematic Jacobians. This approach requires implementation of the kinematic formulas, measurement of the current location of the manipulator and calibration of its kinematic parameters. It is a very complicated method. Basing on the article (Marvel and Falco, 2012) it is claimed that the majority of modern manipulators with force control packages are based on the measurement of force with the use of force sensors in the end-effector, more rarely in the joints. The approaches with force control option in which the force would be determined by the measurements of the position of the end-effector of the manipulator are not present in the writings on this subject matter. This confirms in practice the replacement of indirect force measurement systems by direct force measurement systems.

The author in his works has hitherto analyzed the issue of position/force control of manipulators in interactions with a rigid environment (Gierlak, 2012; Gierlak, 2014; Hendzel et al., 2014). Moreover, the works analyzed the issue of adaptive control of interaction force between the manipulator and a flexible environment assuming that the surface rigidity parameters remain unknown (Gierlak and Szuster, 2017). All those works assumed that the environment surface is continuous and the manipulator constantly contacts the contact surface. This paper expands the approach to this issue when the surface is not continuous and the manipulator periodically loses contact with the environment.

In this paper a combined control strategy which combines two elementary strategies (see: Section 2) has been set forth. The aim of such an approach is to complement one strategy with the second one in situations in which a given elementary strategy applied individually results in unfavourable robot behavior. This allows making use of the advantages of the two elementary strategies and overcoming their disadvantages by means of a fluent passage from one strategy to the other. In order to ensure a proper execution of a strategy, a direct measurement of forces by means of a sensor in the manipulator end-effector was used for the purposes of this paper. Such an approach ensures appropriate fulfillment of the feedback in the force control circuit, even if the surface of the environment is not known exactly. At the same time, the implementation of the combined control strategy requires assuming the nominal geometry of the contact surface (determining theoretical constraints) and the knowledge of the current location of the manipulator end-effector.

The objective of designing the control system presented in the article is: (i) to provide automatic tuning of the system behavior based on the conditions of contact between the manipulator and the surface, (ii) to provide smooth interaction between the manipulator and the surface, (iii) to formulate a control law that is easily interpretable and enables simple selection of amplifications.

The manipulator model is assumed to be a system of rigid bodies and the environment model takes into account the motion resistance in tangential directions and flexibility in normal directions (Section 3). Section 4 discusses the position and combined force control task while taking into account the manipulator and environment models. Section 5 is dedicated to the presentation of a numerical example, which illustrates the operation of the control system. The paper is summarized in Section 6.

2. COMBINED STRATEGY FOR FORCE CONTROL

In the following article, a control strategy which may be referred to as a combined control strategy, since it combines two different control strategies on the basis of competitiveness, has been set forth. One of the component strategies is based on maintaining the desired interaction force together with the desired motion velocity, whereas the trajectory is automatically adjusted to the shape of the surface. The second component strategy is based on executing the desired trajectory regardless of the shape of the processed surface. A combination of these strategies on the basis of competitiveness introduces to some extent a compromise between them, which means that the requirements of each strategy are conducted in a „soft” way. The proposed method may converge with either of the strategies depending on the introduced project coefficient. The principles of operation of the component control strategies and the result of their competitive combination is

presented in Fig. 2. The combined strategy in question is not a combination of the two discussed strategies used in commercial and industrial applications. The first elementary strategy in fact corresponds with the strategy used in commercial and industrial applications (Fig. 1a), it also has strong theoretical foundations and it is widely discussed in the professional literature on this subject-matter; nonetheless, the second elementary strategy does not correspond with the presented commercial application (Fig. 1b). It derives from position control methods and it aims at executing a trajectory in order to ensure an appropriate shape of the surface.

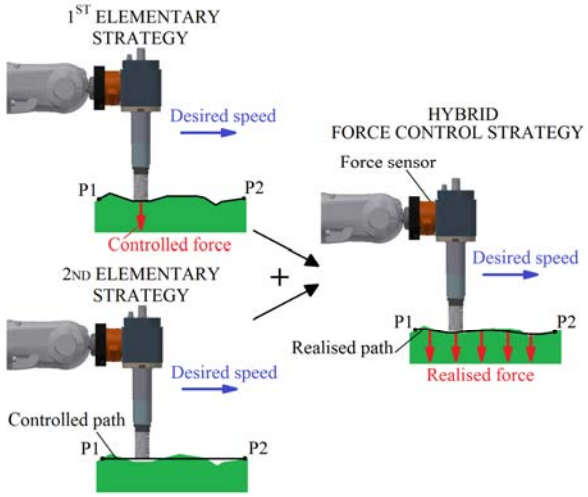

Fig. 2. Combined strategy for force control.

If a theoretical description of the environment and the desired trajectory in a normal direction resulting from the said description corresponds with the actual environment shape, the first elementary strategy is executed. It is an extreme example of the system operation and the control is concerned only with controlling the clamping force only in the normal direction towards the surface. If the shape of the environment diverges from theoretical assumptions, the importance of the second elementary strategy is consequently stressed, the activity of which depends on the difference between the desired trajectory and the real trajectory in the normal direction. It is worth noticing that in the case the actual environment is different from theoretical assumptions, competition between the two elementary strategies occurs. The control system automatically enforces the balance between the strategies and none of them will be fully executed. This protects the system from an "extreme" activity of each strategy and the disadvantages of the elementary strategies do not appear, although they would if they were applied individually.

3. MANIPULATOR AND ENVIRONMENT MODEL

While implementing the simplest methods of force control known from the literature on this subject-matter, which are based on assuming infinite stiffness of the environment, very important features of mechanical systems, which influence both the dynamics of the system and the quality of executing the control strategy, are not taken into account. Hence in the herein discussed approach to the description of the dynamics of the system, the flexibility of the environment, which is a significant aspect in the field of robotized machining, has been taken into account. This in fact complicates the system description, yet it allows real description of this subject-matter and achieving results which are close to reality.

Dynamics equation of motion of the manipulator in the joint space takes the form (Lewis et al. (1999))

$$M(q)\ddot{q} + C(q,\dot{q})\dot{q} + F(\dot{q}) + G(q) = u + J(q)^T\lambda \tag{1}$$

where $q \in R^n$ is the vector of generalized coordinates, $M(q) \in R^{n\times n}$ is the inertia matrix, $C(q,\dot{q})\dot{q} \in R^n$ is the vector of centrifugal and Coriolis forces (moments), $F(\dot{q}) \in R^n$ is the viscous friction vector, $G(q) \in R^n$ is the gravity vector, $u \in R^n$ is the control input vector, $J(q) \in R^{m\times n}$ is an analytical Jacobian matrix, $\lambda \in R^m$ is an interaction force vector expressed in the task space, n is the number of degrees of freedom of the manipulator, m is a task space dimension.

The manipulator's workspace is associated with the Cartesian coordinate system. The kinematics of the manipulator in the Cartesian coordinates c is described by the function

$$c = k(q) \in R^m. \tag{2}$$

The relationship between velocity in the Cartesian space and in joint space is as follows

$$\dot{c} = J\dot{q} \tag{3}$$

where the analytical Jacobian J is

$$J = \partial c/\partial q = \partial k(q)/\partial q. \tag{4}$$

On the basis of (3) the acceleration takes the form

$$\ddot{c} = \dot{J}\dot{q} + J\ddot{q}. \tag{5}$$

Dependencies (1), (3), (4), and (5) permit to represent the dynamics of the manipulator in the Cartesian coordinates $\{C\}$. It will be a convenient form of description of the position-force control taking into account the characteristics of the environment with which the robot interacts. For this purpose (1) was premultiplied by $(J^T)^{-1}$, in order that the interactive force λ may be expressed directly in the Cartesian coordinates:

$$J^{-T}[M(q)\ddot{q} + C(q,\dot{q})\dot{q} + F(\dot{q}) + G(q)] = J^{-T}u + \lambda \tag{6}$$

where was taken into account that $(J^T)^{-1} = (J^{-1})^T$ which was written in short form as J^{-T}. On the basis of (3) and (5) it was determined

$$\dot{q} = J^{-1}\dot{c}, \tag{7}$$

$$\ddot{q} = J^{-1}\ddot{c} - J^{-1}\dot{J}J^{-1}\dot{c}, \tag{8}$$

and substituted into (6), which took the form of

$$J^{-T}M(q)J^{-1}\ddot{c} + [J^{-T}C(q,\dot{q})J^{-1} - J^{-T}M(q)J^{-1}\dot{J}J^{-1}]\dot{c} + J^{-T}[F(\dot{q}) + G(q)] = J^{-T}u + \lambda. \tag{9}$$

Assumed designations

$$\left.\begin{array}{c} J^{-T}M(q)J^{-1} = (JM(q)^{-1}J^T)^{-1} = A(q) \in R^{m\times m} \\ J^{-T}C(q,\dot{q})J^{-1} - J^{-T}M(q)J^{-1}\dot{J}J^{-1} = \\ J^{-T}C(q,\dot{q})J^{-1} - A(q)\dot{J}J^{-1} = H(q,\dot{q}) \in R^{m\times m} \\ J^{-T}[F(\dot{q}) + G(q)] = B(q,\dot{q}) \in R^m \\ J^{-T}u = U \in R^m \end{array}\right\} \tag{10}$$

and the dynamics of the manipulator were expressed in the Cartesian space in the form of (Canudas et al., 1996; Lewis et al., 1993)

$$A(q)\ddot{c} + H(q,\dot{q})\dot{c} + B(q,\dot{q}) = U + \lambda. \quad (11)$$

Divide the m-dimensional space of the Cartesian coordinates $\{C\}$ to subspace $\{T\}$ and $\{N\}$: $\{C\} = \{T\} \oplus \{N\}$ (Vukobratovič et al., 2002). Subspace $\{N\}$ is an r-dimensional space of directions n_i normal to the contact surface of the manipulator's end-effector and the environment, whereas subspace $\{T\}$ is $(m-r)$-dimensional space of tangent directions τ_i. Therefore the vector c can be written as

$$c = [c_\tau^T \quad c_n^T]^T \quad (12)$$

where $c_\tau \in R^{m-r}$, $c_n \in R^r$. Assuming that the environment, with which the manipulator enters contact (through the end-effector) is characterized by elasticity, then the said environment feature is present in the subspace $\{N\}$. The environment will be described by the equation:

$$K_e c_n = F_{en} \quad (13)$$

where $K_e \in R^{r\times r}$ is a diagonal matrix of stiffness of the environment, that meets the dependency $K_e = K_e^T > 0$.

In the tangential direction, the movement of the end-effector of manipulator over the contact surface will be accompanied by resistance. It is modeled with dry friction. In the case of translation in the contact plane the elements of the vector $F_{e\tau}$ will take the form:

$$F_{e\tau(.)} = \mu F_{en(.)} sign(v_{\tau(.)}) \quad (14)$$

where $F_{e\tau(.)}$, $F_{en(.)}$ are appropriate components of tangential and normal force, μ is the coefficient of dry friction, $v_{\tau(.)}$ is the velocity of movement along the direction $\tau(.)$. However, in the instance of rotation in the contact plane the elements of vector $F_{e\tau}$ will take the form:

$$F_{e\tau(.)} = \mu_Z F_{en(.)} sign(\omega_{n(.)}) \quad (15)$$

where: $F_{e\tau(.)}$, $F_{en(.)}$ are appropriate components of the tangential and normal force, in this instance $F_{e\tau(.)}$ will be the momentum of resistance forces, μ_Z is a substitute coefficient of dry friction, $\omega_{n(.)}$ is an angular velocity of rotation in the contact plane, that is the turnover around the axis $n(.)$.

In relation to the above dissertations, the interaction force vector can be written as

$$\lambda = [-F_{e\tau}^T \quad -F_{en}^T]^T \quad (16)$$

where $F_{e\tau} \in R^{m-r}$ is a vector of tangential forces, $F_{en} \in R^r$ is a vector of normal forces.

On the basis of (13) the formula is receive:

$$c_n = P_e F_{en} \quad (17)$$

where $P_e = K_e^{-1} \in R^{r\times r}$ is the environmental flexibility matrix, which is the diagonal matrix, hence the dependence of $P_e = P_e^T > 0$ arises. Taking into account (17) in (12), and then in (11), the following equation is obtain

$$A(q)\begin{bmatrix}\ddot{c}_\tau \\ P_e\ddot{F}_{e\,n}\end{bmatrix} + H(q,\dot{q})\begin{bmatrix}\dot{c}_\tau \\ P_e\dot{F}_{e\,n}\end{bmatrix} + B(q,\dot{q}) = U + \lambda \quad (18)$$

or

$$A(q)E\ddot{\theta} + H(q,\dot{q})E\dot{\theta} + B(q,\dot{q}) = U + \lambda \quad (19)$$

where

$$\theta = \begin{bmatrix}c_\tau \\ F_{e\,n}\end{bmatrix} \in R^m, \quad (20)$$

$$E = \begin{bmatrix}I_{(m-r)\times(m-r)} & 0 \\ 0 & P_e\end{bmatrix} \in R^{m\times m}. \quad (21)$$

Equation (19) describes the dynamics of the system in Cartesian space as a function of movement parameters in the tangent plane and the forces on the normal directions. This mathematical model bears the structural qualities of stiff manipulator models as set forth by (Canudas et al., 1996).

4. THE FUNDAMENTALS OF POSITION-FORCE CONTROL WITH THE USE OF COMBINED CONTROL OF INTERACTION FORCE

In terms of the theory of control, the execution of the motion of a manipulator during its interaction with the environment is understood as control of a system with constraints. These constraints result from the shape of the environment surface and they are referred to as constraints that limit the movement of the system. They generate reactions, that is, interaction forces, which may be controlled. This allows executing a selected strategy for force control.

The presented control algorithm is based on assuming the knowledge of the environment surface and system dynamics. Thus, let the dynamics of the system (19) and:

- nominal trajectory of the manipulator end-effector in normal direction $c_{n\,nom}(t) \in R^r$ and its derivative, that is, the motion velocity $\dot{c}_{n\,nom}(t)$, which result from the assumed shape of the environment,

- motion trajectory of the manipulator end-effector in tangential direction $c_{\tau d}(t) \in R^{m-r}$, $\dot{c}_{\tau d}(t)$, $\ddot{c}_{\tau d}(t)$,

- desired force in n-direction $F_{en_d}(t) \in R^r$, $\dot{F}_{en_d}(t)$, $\ddot{F}_{en_d}(t)$.

A control, that ensures execution the desired motion and force trajectories in the form of

$$U = A(q)\beta + H(q,\dot{q})E\dot{\theta} + B(q,\dot{q}) + F_C \quad (22)$$

was taken, in which $H(q,\dot{q})E\dot{\theta} + B(q,\dot{q})$ is supposed to compensate for non-linearity. The unit $\beta \in R^m$ selected as

$$\beta = \begin{bmatrix}\ddot{c}_{\tau d} + K_V\dot{\tilde{c}}_\tau + K_P\tilde{c}_\tau \\ K_e^{-1}\ddot{F}_{en}\end{bmatrix} \quad (23)$$

is responsible for minimizing the motion error in the tangential direction and compensating for the influence of the environment in the normal direction. The matrices $K_P \in R^{(m-r)\times(m-r)}$ and $K_V \in R^{(m-r)\times(m-r)}$ are the matrices of direct proportion and differential amplifications in the position control circuit. The error of motion in the tangential direction is marked as

$$\tilde{c}_\tau = c_{\tau d} - c_\tau, \quad (24)$$

whereas $F_C \in R^m$ is force control selected in the form of

$$F_C = [F_{e\tau}^T \quad U_F^T]^T. \tag{25}$$

Part of the control $F_{e\tau}$ is responsible for compensating for the resistance forces in tangential direction, whereas the term

$$U_F = U_n - U_v \tag{26}$$

aims at executing combined force control. The term

$$U_n = K_{FP}\tilde{F}_{en} + K_{FV}\dot{\tilde{F}}_{en} \tag{27}$$

has been introduced in order to execute the first elementary strategy, that is, minimizing the error of interaction force in normal direction, in which $K_{FP} \in R^{r\times r}$ is a matrix of proportional force gain, $K_{FV} \in R^{r\times r}$ is a matrix of differential force gain, whereas

$$\tilde{F}_{en} = F_{en_d} - F_{en} \tag{28}$$

is the error of executing force in normal direction. The unit U_v creates a situation in which in the case of differences between theoretical constraints and real constraints, the manipulator end-effector does not diverge from theoretical constraints significantly. It is the control which aims at executing the desired trajectory in the normal direction, thus it executes the second elementary strategy. The unit U_v may be interpreted in terms of mechanical systems in an interesting way. It may be understood as a virtual resistance force, which substitutes the reaction of real system constraints in the case when manipulator loses contact with these constraints, e.g. due to surface irregularities. The form of this part of control is based on the model of elastic and viscous resistances as follows:

$$U_v = K_k\xi + K_c\dot{\xi}, \tag{29}$$

in which $K_k \in R^{r\times r}$ and $K_c \in R^{r\times r}$ are diagonal gain matrices, which may be interpreted as coefficients of virtual spring and viscous resistances. The value $\xi \in R^r$ defined as

$$\xi = c_n - \xi_0 - c_{n\,nom} \tag{30}$$

is connected with the difference between nominal position of the manipulator end-effector $c_{n\,nom}$ which results from theoretically existing constraints and the real position c_n in the normal direction. In other words ξ is the measure of the displacement of the manipulator end-effector with regard to the assumed constraints in a normal direction. To put it in detail, it is necessary to add that the formula $\xi_0 = K_e^{-1}F_{en_d}$ takes into account the environment deformation resulting from the clamping force F_{en}. In the case of high environment stiffness, this deformation is not significant, but in the case of more susceptible elements, it is necessary to take it into account. The discussed issue is presented in Fig. 3. A situation in which in a certain area the real constraints correspond with the theoretical constraints, an in the other area they differ significantly (Fig. 3a). If the real constraints correspond with the theoretical constraints, the sum $\xi_0 + c_{n\,nom}$ is equal to c_n and the control value $U_v = 0$ (Fig. 3b). Nonetheless, if the real constraints do not correspond with the theoretical constraints, the sum $\xi_0 + c_{n\,nom}$ is not equal to c_n and the control U_v becomes activated (Fig. 3c), which may be interpreted as the force of virtual constraints reaction of K_k stiffness and K_c damping. As shown in Fig. 3c, in the area in which there are no natural manipulator constraints, there is no constraints reaction as well. An attempt to execute the first elementary strategy would result in rapid acceleration of the manipulator end-effector until it hits the surface of constraints in the fault zone impetuously. Activating the second strategy in this area results in generating contrary control, which substitutes the activity of the constraints reaction force and is referred to as the reaction of virtual constraints. This results in the motion of the manipulator end-effector in the proximity of the theoretical constraints and a fluent passage "over the fault zone". A similar problem of modification of the manipulator trajectory in the presence of obstacles in the proximity of points of contact with the environment, based on the measurement of forces was described by (Capisani and Ferrara, 2012).

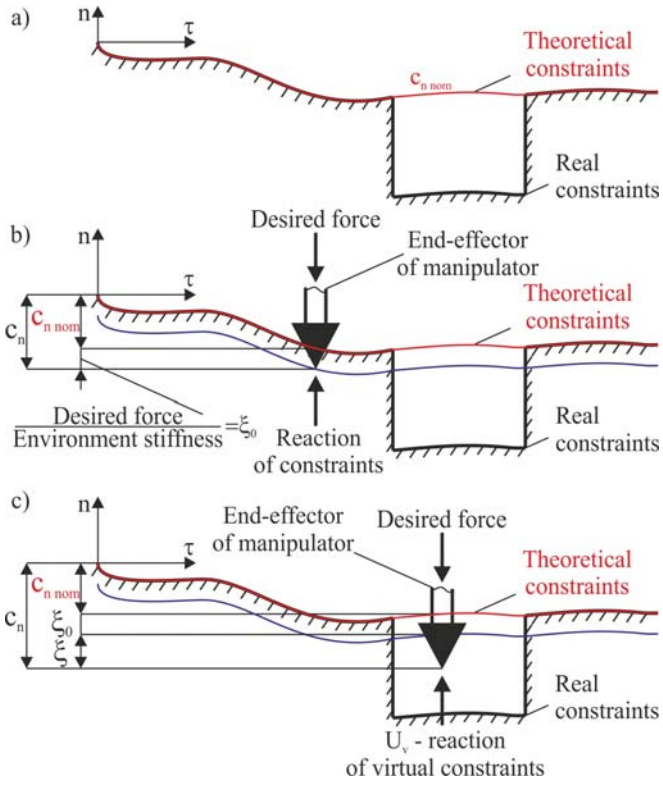

Fig. 3. Manipulator constraints.

Taking into account (22)-(30) and (16) in (19), the formula

$$A(q)\left(E\ddot{\theta} - \beta\right) = \begin{bmatrix} 0 \\ U_n - U_v \end{bmatrix} \tag{31}$$

was arrived at and then taking into account (20) and (21) and by putting it in order, a description of a closed-loop system

$$A(q)\begin{bmatrix} \ddot{\tilde{c}}_\tau + K_V\dot{\tilde{c}}_\tau + K_P\tilde{c}_\tau \\ -P_e\ddot{F}_{en} + K_e^{-1}\ddot{F}_{en} \end{bmatrix} + \begin{bmatrix} 0 \\ U_n - U_v \end{bmatrix} = 0 \tag{32}$$

was arrived at. In the case of a precisely known matrix K_e^{-1} occurring in the control law, it shall be $-P_e\ddot{F}_{en} + K_e^{-1}\ddot{F}_{en} = 0$ which eventually results in the following formula

$$A(q)\begin{bmatrix} \ddot{\tilde{c}}_\tau + K_V\dot{\tilde{c}}_\tau + K_P\tilde{c}_\tau \\ 0 \end{bmatrix} + \begin{bmatrix} 0 \\ U_n - U_v \end{bmatrix} = 0. \tag{33}$$

The equation (33) may be as well put in the following form

$$\begin{cases} A_{11}(q)\left(\ddot{\tilde{c}}_{\tau} + K_V\dot{\tilde{c}}_{\tau} + K_P\tilde{c}_{\tau}\right) = 0 \\ A_{21}(q)\left(\ddot{\tilde{c}}_{\tau} + K_V\dot{\tilde{c}}_{\tau} + K_P\tilde{c}_{\tau}\right) + U_n - U_v = 0 \end{cases}, \quad (34)$$

in which

$$A_{11}(q) = E_1^T A(q) E_1 \in R^{(m-r)\times(m-r)}, \quad (35)$$

$$A_{21}(q) = E_2^T A(q) E_1 \in R^{r\times(m-r)}, \quad (36)$$

$$E_1 = \begin{bmatrix} I_{m-r} \\ 0 \end{bmatrix} \in R^{m\times(m-r)}, \quad E_2 = \begin{bmatrix} 0 \\ I_r \end{bmatrix} \in R^{m\times r}. \quad (37)$$

The system stability will be demonstrated by means of analysis of open solutions of equations of the closed-loop system. The analysis of the first equation of (34) aims at demonstrating the motion stability in tangential direction, whereas the analysis of the second equation of (34) allows demonstrating stability of the elementary strategies and the combined force control strategy in normal direction.

Theorem. For limited elements of the $A_{11}(q)$ matrix, the error of motion $\tilde{c}_{\tau}$ and their derivatives shall be asymptotically convergent to zero, in the case of selection of K_P and K_V matrices as diagonal matrices, the elements of which in the diagonal shall meet the condition

$$(k_{Vi}/2)^2 \geq k_{Pi} > 0, \quad i = 1, \ldots, m-r. \quad (38)$$

Proof. The first equation of (34) will be fulfilled for limited elements of the $A_{11}(q)$ matrix if

$$\ddot{\tilde{c}}_{\tau} + K_V\dot{\tilde{c}}_{\tau} + K_P\tilde{c}_{\tau} = 0. \quad (39)$$

The equation (39) is the system of $(m-r)$ linear second-order homogeneous differential equations of constant coefficients. These coefficients are the proportional gain k_{Pi} and the differential gain k_{Vi} grouped in the K_P and K_V project matrices diagonals. The solution of (39) depends on the values of these coefficients. The solution will be stable and asymptotically divergent to zero for appropriately selected matrices K_P and K_V. It is necessary to analyze the solutions of (39) for non-zero initial conditions:

$$\begin{cases} \tilde{c}_{\tau i}(t=0) = \tilde{c}_{\tau i0} \\ \dot{\tilde{c}}_{\tau i}(t=0) = \dot{\tilde{c}}_{\tau i0} \end{cases}, \quad i = 1, \ldots, m-r. \quad (40)$$

The solutions of (39) have the form of

$$\tilde{c}_{\tau i} = R_i e^{\alpha t}. \quad (41)$$

Upon substituting (41) to (39), the $(m-r)$ of equations in the following form was obtained:

$$R_i e^{\alpha t}(\alpha_i^2 + k_{Vi}\alpha_i + k_{Pi}) = 0, \quad (42)$$

in which

$$\alpha_i^2 + k_{Vi}\alpha_i + k_{Pi} = 0 \quad (43)$$

is the i-th characteristic equation, the solution of which are referred to as the characteristic roots. The solution (41) shall be of non-oscillational character, if the characteristic roots are real, i.e. $(k_{Vi}/2)^2 \geq k_{Pi}$. Then the solution of (40) is

$$\alpha_{i1,i2} = -k_{Vi}/2 \mp \sqrt{(k_{Vi}/2)^2 - k_{Pi}}. \quad (44)$$

Both coefficients α_{i1} and α_{i2} are negative if $k_{Pi} > 0$. Then the solution (41) will be asymptotically divergent to zero. This implies fulfilling of (39) and the first equation of (34).

The analysis of the second equation of (34) is presented hereinunder. Taking into account (39), it was put that

$$U_n - U_v = 0. \quad (45)$$

The equation (45) presents the sum of control for the two basic control strategies. In order to explain the stability of combined control, three cases will be discussed: two extreme cases in which basic control strategies are executed separately and an intermediate case, in which the strategies are executed simultaneously. Such an approach allows deep understanding of how the system operates.

Case 1. If the manipulator maintains contact with the surface and conducts the nominal trajectory $c_{n\,nom}$ taking into account the displacement $\xi_0 = K_e^{-1}F_{en_d}$ and the velocity $\dot{c}_{n\,nom}$ taking into account $\dot{\xi}_0 = K_e^{-1}\dot{F}_{en_d}$ in the normal direction resulting from the shape of the surface, the control $U_v = 0$. Hence the equation (45) that describes the dynamics in the normal direction has the form of

$$\dot{\tilde{F}}_{en} + K_{FV}^{-1}K_{FP}\tilde{F}_{en} = 0. \quad (46)$$

The equation (46) is the system of r linear first-order homogeneous differential equations with constant coefficients, which can be written as

$$\dot{\tilde{F}}_{enj} + k_{FPj}/k_{FVj}\tilde{F}_{enj} = 0, \quad j = 1, \ldots, r. \quad (47)$$

Each of the equations of (47) has one eigenvalue and the solution of the equations asymptotically converges with zero if the eigenvalue is negative, that is, if $k_{FPj}/k_{FVj} > 0$, where k_{FPj}/k_{FVj} are the elements in the $K_{FV}^{-1}K_{FP}$ matrix diagonal. Solution of (47) has a form

$$\tilde{F}_{enj} = C_j \exp(-k_{FPj}/k_{FVj}t). \quad (48)$$

The initial value of the force error is $\tilde{F}_{enj}(0) = F_{enj_d}(0) - F_{enj}(0) = F_{enj_d}(0)$ because $F_{enj}(0) = 0$. By taking into account the initial conditions in the equation (48), $C_j = F_{enj_d}(0)$ was arrived at. Since the error $\tilde{F}_{en}$ converges with zero, then $F_{enj} \to F_{enj_d}$ according to the equation

$$F_{enj} = F_{enj_d} - F_{enj_d}(0)\exp(-k_{FPj}/k_{FVj}t), \quad (49)$$

whereas, the position of the end-effector determined on the basis of (13) is described as

$$c_{nj} = 1/k_{ej}\left[F_{enj_d} - F_{enj_d}(0)\exp(-k_{FPj}/k_{FVj}t)\right] \quad (50)$$

and $c_{nj} \to F_{enj_d}/k_{ej}$ for $t \to \infty$, i.e. the solution is limited.

Case 2. If the manipulator does not contact the surface, the interaction force is $F_{en} = 0$ and a displacement from the nominal trajectory in the normal direction occurs. The control U_v is activated and the equation describing the balance of forces in a normal direction has the form of

$$K_{FP}F_{en_d} + K_{FV}\dot{F}_{en_d} - K_k\xi - K_c\dot{\xi} = 0. \quad (51)$$

The result is that the dynamics of the ξ error is stimulated only by the desired trajectory which is limited, so $\dot{\xi}$ will be limited as well. This is all that could be inferred from the

theoretical analysis. Bearing in mind the practical aspects, it is necessary to state that in technical applications, both of the velocities of changes of forces $\dot{F}_{en_d}$ as well as the amplifications K_{FV} are small, thus the significance of the term $K_{FV}\dot{F}_{en_d}$ in (51) is usually minor. This means that the main stimulus for the ξ error is the force F_{en_d}, which for slow changes is approximately $F_{en_d} \sim const$. Then the system of r linear first-order non-homogeneous differential equations of constant coefficients may be analyzed

$$K_c\dot{\xi} + K_k\xi = K_{FP}F_{en_d}. \tag{52}$$

Each of these equations may be put in the form of

$$\dot{\xi}_j + (k_{kj}/k_{cj})\xi_j = (k_{FPj}/k_{cj})F_{enj_d},\ j = 1, \dots, r, \tag{53}$$

in which k_{kj} and k_{cj} are the element of matrices K_k and K_c. For zero initial conditions its solution has the form of

$$\xi_j = F_{enj_d}/k_{kj}\left[1 - \exp\left(-k_{kj}/k_{cj}t\right)\right]. \tag{54}$$

If $t \to \infty$ then the deviation in normal direction $\xi_j \to F_{enj_d}/k_{kj}$, thus the deviation tends asymptotically from zero to a constant value. It is noticeable, that the error $\xi_j \to \infty$ for $k_{kj} = 0$, whereas it is reduced in accordance with the increase of the coefficient k_{kj}. The speed of deviation may be determined by differentiating the equation (54)

$$\dot{\xi}_j = F_{enj_d}/k_{cj}\exp\left(-k_{kj}/k_{cj}t\right) \tag{55}$$

and tends asymptotically from F_{enj_d}/k_{cj} to zero if $t \to \infty$. The maximal speed of deviation value may be reduced by increasing the damping factor k_{cj}.

Case 3. If two elementary strategies are executed simultaneously, thus the combined control is executed, the behavior of the system in the normal direction is described by (45), which - upon taking into account the controls (27) and (29) - has the form of

$$K_{FP}\tilde{F}_{en} + K_{FV}\dot{\tilde{F}}_{en} - K_k\xi - K_c\dot{\xi} = 0. \tag{56}$$

Such a situation occurs if the manipulator maintains contact with the surface of the environment, but the shape of this environment fails to correspond with the nominal trajectory $c_{n\,nom}$. This situation is shown in Fig. 4. In the equation (56), two variables, $\tilde{F}_{en}$ and ξ which are dependent on each other are present, thus the force error $\tilde{F}_{en}$ may be expressed in the function ξ. The transformations shall be made in order to achieve it. First of all, it is necessary to notice that the value of force in the case in question is

$$F_{en} = K_e(c_n - c_{n\,nom} - h), \tag{57}$$

in which h is the value characterizing the imprecision of the actual surface of the constraints assumed as $h = const.$, whereas the value of the desired force may be put as $F_{en_d} = K_e\xi_0$. The interaction force error on the basis of (28) has been put in the form of

$$\tilde{F}_{en} = K_e\xi_0 - K_e(c_n - c_{n\,nom} - h) = K_e(h - \xi), \tag{58}$$

in which (30) was used. Substituting the equation (58) to (56) results in the equation

$$(K_{FV}K_e + K_c)\dot{\xi} + (K_{FP}K_e + K_k)\xi = K_{FP}K_eh, \tag{59}$$

which is the system of r linear first-order non-homogeneous differential equations of constant coefficients. Each of these equations may be put in the form of

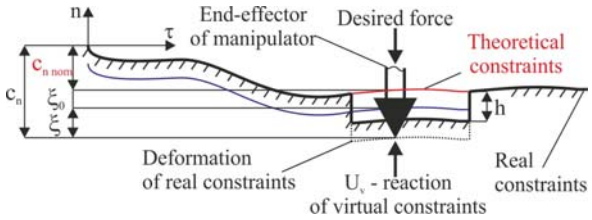

Fig. 4. Combined strategy in case of surface inaccuracies.

$$\dot{\xi}_j + \frac{k_{FPj}k_{ej}+k_{kj}}{k_{FVj}k_{ej}+k_{cj}}\xi_j = \frac{k_{ej}}{k_{FVj}k_{ej}+k_{cj}}h_j,\ j = 1, \dots, r. \tag{60}$$

The equation (60) was solved analogically to (53), so for zero initial conditions $\xi_j(0) = 0$, the displacement in the normal direction

$$\xi_j = h_j\frac{k_{ej}}{k_{FPj}k_{ej}+k_{kj}}\left[1 - exp\left(-\frac{k_{FPj}k_{ej}+k_{kj}}{k_{FVj}k_{ej}+k_{cj}}t\right)\right] \tag{61}$$

was arrived at. If $t \to \infty$ then $\xi_j \to h_jk_{ej}/(k_{FPj}k_{ej} + k_{kj})$, thus the deviation tends asymptotically from zero to a constant value. It is noticeable that the displacement $\xi_j = h_j$ for $k_{kj} = 0$, yet it is reduced along with the increase of the coefficient k_{kj}. The dependence of error ξ_j on environment rigidity and amplification k_{kj} in a steady state is presented in Fig. 5. The behavior of the system in the coordinates c_{nj} which describe the displacement in the normal direction may be specified as well. On the basis of (30) it may be put that in the state determined for $t \to \infty$ it will be

$$c_{nj} = h_jk_{ej}(k_{FPj}k_{ej} + k_{kj}) + \xi_{0j} + c_{nj\,nom}, \tag{62}$$

in which $\xi_{0j} = F_{enj_d}/k_{ej}$. It is also worth to show how in this situation the interaction force described by means of (57) is executed. In the j-th direction, this force has the form of

$$F_{enj} = k_{ej}\left(c_{nj} - c_{nj\,nom} - h_j\right) \tag{63}$$

and upon taking into account the relation $\xi_{0j} = F_{enj_d}/k_{ej}$ and (62) the equation

$$F_{enj} = k_{ej}h_j\frac{(1-k_{FPj})k_{ej}-k_{kj}}{k_{FPj}k_{ej}+k_{kj}} + F_{enj_d} \tag{64}$$

was arrived at. On the basis of (62) and (64) it may be said that for $k_{kj} = 0$ and $k_{FPj} = 1$ the manipulator end-effector will move along the surface with additional displacement ξ_{0j} devoid of the nominal trajectory in the normal direction, that is, $c_{nj} = h_j + \xi_{0j} + c_{nj\,nom}$ whereas the interaction force will be equal to $F_{enj} = F_{enj_d}$. On the other hand, for $k_{kj} \to \infty$, the manipulator end-effector will move along the nominal trajectory with the displacement ξ_{0j} regardless of the environment surface, that is, $c_{nj} = \xi_{0j} + c_{nj\,nom}$, whereas the interaction force will be $F_{enj} = F_{enj_d} - k_{ej}h_j$. The latter

theorem is valid for $F_{enj_d} \geq k_{ej}h_j$, as for significant imprecisions of the surface, the value h_j is big enough, so that $F_{enj_d} < k_{ej}h_j$ and then $F_{enj} = 0$ because there is no contact between the manipulator and the environment. Each intermediary value $k_{kj} \in (0, \infty)$ introduces a compromise between these two extreme solutions. Based on (28) and (64), the characteristics of the force error in the function of environment rigidity and amplification k_{kj} for $k_{FPj} = 1$ in a steady state have been identified (Fig. 6). Obviously, force and position errors cannot be simultaneously reduced if a surface inaccuracy occurs. The dependence between these errors in a steady state is defined as $\tilde{F}_{enj} = k_{ej}(h_j - \xi_j)$ based on (58). It is shown in Fig. 7. By selecting amplification k_{kj}, one or the other error is reduced.

To sum up, it may be concluded that both in the case the real constraints correspond with theoretical constraints and in the case of significant imprecisions of real constraints, or even in the event of the lack of constraints, the solution of the closed-loop system equations remain stable. Moreover, for an appropriately high amplification $K_k = diag\{k_{kj}\}$, the error ξ may be very little. As shown in the following section, the amplification K_k is the essential parameter having influence on the execution of the combined strategy for force control.

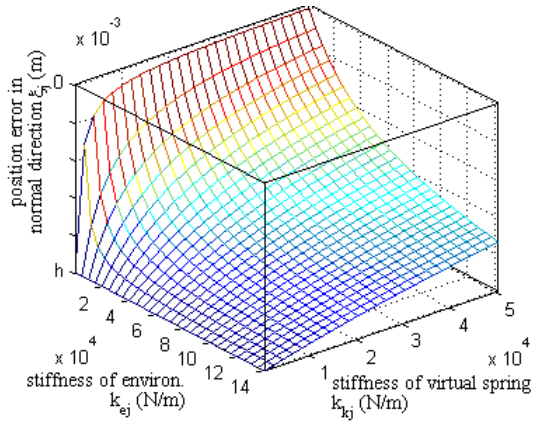

Fig. 5. Characteristics of position error ξ_j.

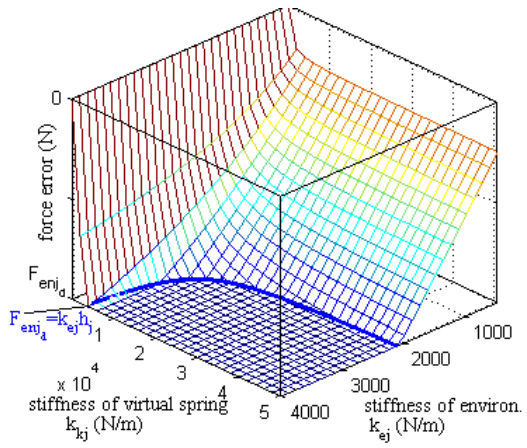

Fig. 6. Characteristics of force error $\tilde{F}_{enj}$.

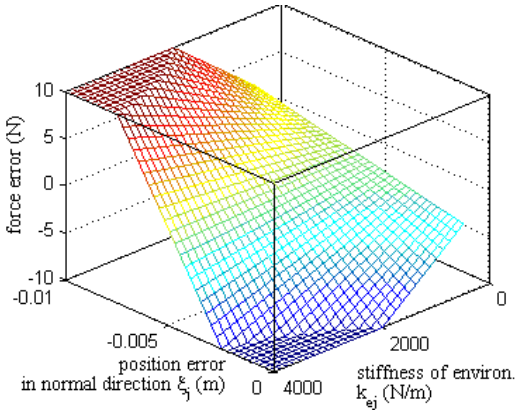

Fig. 7. Dependence of the force error on the position error.

The methodology described in this section is based on the theory commonly functioning in mechanics. The analysis of open forms of solutions of linearized system equations was conducted intentionally, taking additionally simplifications. This allows understanding the behavior of the system and the principles of control system operation.

5. NUMERICAL EXAMPLE

As an example, let's consider control of a two-link planar manipulator (Fig. 8) whose dynamics in joint coordinates is described by (1), in which the matrixes and vectors are as follows (Gierlak and Szuster, 2017).

$$M(q) = \begin{bmatrix} a_1 & a_2 cos(q_2 - q_1) \\ a_2 cos(q_2 - q_1) & a_3 \end{bmatrix}, \tag{65}$$

$$C(q, \dot{q}) = \begin{bmatrix} 0 & -a_2 sin(q_2 - q_1)\dot{q}_2 \\ a_2 sin(q_2 - q_1)\dot{q}_1 & 0 \end{bmatrix}, \tag{66}$$

$$F(\dot{q}) = [a_4\dot{q}_1 \quad a_5\dot{q}_2]^T, \tag{67}$$

$$G(q) = [a_6 \cos(q_1) \quad a_7 \cos(q_2)]^T, \tag{68}$$

$$u = [u_1 \quad u_2]^T, \tag{69}$$

$$q = [q_1 \quad q_2]^T. \tag{70}$$

The parameters in matrixes are as follows:

$$\begin{cases} a_1 = l_{c1}^2 m_1 + l_1^2 m_2 + I_1; \ a_2 = l_1 l_{c2} m_2; \\ a_3 = l_{c2}^2 m_2 + I_2; \ a_4 = c_{v1}; \ a_5 = c_{v2}; \\ a_6 = (l_{c1} m_1 + l_1 m_2) g; \ a_7 = l_{c2} m_2 g \end{cases} \tag{71}$$

where: m_i is a mass of i-th link, l_i is a length of i-th link, l_{ci} is the distance between center of mass of i-th link and end of $(i-1)$ link, I_i is a mass moment of inertia of i-th link relative to its center of mass, c_{vi} is coefficient of viscous friction in i-th kinematic pair. The parameter values are shown in Table 1. The manipulator end-effector's position in Cartesian space is:

$$c = \begin{bmatrix} c_{\tau 1} \\ c_{n1} \end{bmatrix} = \begin{bmatrix} l_1 cos(q_1) + l_2 cos(q_2) \\ l_1 sin(q_1) + l_2 sin(q_2) \end{bmatrix}. \tag{72}$$

The analytical Jacobian (4) for the manipulator is:

$$J = \begin{bmatrix} -l_1 sin(q_1) & -l_2 sin(q_2) \\ l_1 cos(q_1) & l_2 cos(q_2) \end{bmatrix}. \tag{73}$$

The equation describing the dynamics of the manipulator in Cartesian coordinates is (19), where $A(q)$, $H(q, \dot{q})$, $B(q, \dot{q})$, and U are defined by (10) and

$$\lambda = [-F_{e\tau 1} \quad -F_{en1}]^T = [-\mu F_{en1} sgn(\dot{c}_{\tau 1}) \quad -F_{en1}]^T, \quad (74)$$

$$E = \begin{bmatrix} 1 & 0 \\ 0 & P_{e1} \end{bmatrix}, \quad (75)$$

$$\theta = [c_{\tau 1} \quad F_{en1}]^T. \quad (76)$$

In the analyzed case a geometry of the contact surface which corresponds with the tangent axis was assumed, hence $c_{n1\,nom}(t) = const. = 0$, $\dot{c}_{n1\,nom}(t) = 0$. A constant down force towards the surface was assumed, so the trajectory of force in a normal direction is $F_{en1_d}(t) = F_{e1\,max} = const.$, $\dot{F}_{en1_d}(t) = 0$, $\ddot{F}_{en1_d}(t) = 0$. Due to flexibility, in the normal

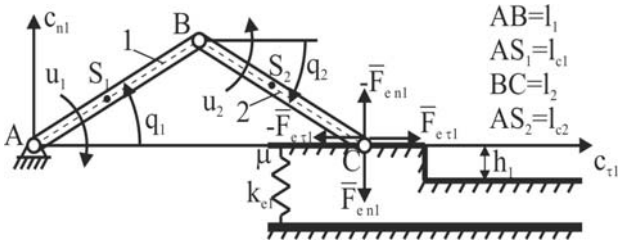

Fig. 8. The scheme of the 2-degrees-of-freedom manipulator with environment.

direction the surface deformation of $\xi_{01} = F_{en1_d}/k_{e1}$ will occur. The trajectory in the tangent direction was assumed in a way which allows limiting displacement, velocity and acceleration. The displacement is described by the function

$$c_{\tau 1d} = c_0 + \frac{v_{max}}{w_\tau}\left[ln\frac{exp(w_\tau(t-t_{c1}))+1}{exp(w_\tau(t-t_{c2}))+1} + ln\frac{exp(w_\tau(t-t_{c4}))+1}{exp(w_\tau(t-t_{c3}))+1}\right] \quad (77)$$

where $c_0 = c_{\tau 1d}(0)$ is the initial position of the end-effector, v_{max} is the maximum velocity, w_τ is the coefficient corresponding to the velocity increase and decrease rate. In Fig. 9 the theoretical constraints, the nominal path and real constraints (Fig. 9a) and the desired displacement along the tangential direction (Fig. 9b) are shown. In the selection of actual constraints, selected guidelines presented in (Bruhm et al., 2015) have been applied. Parameters of the desired trajectory are shown in Table 1.

5.1 Analytical solutions – case studies

In the following subsection the results of research into the influence of coefficients in the control system on the behavior of the system is presented. The influence of the coefficients k_{k1} and k_{c1} on the implementation of the combined force control strategy was researched in particular. Environment parameters and control system parameters for linear system used in the simulation study are as follows: $k_{e1} = 1000$ (N/m), $h_1 = -0.005$ (m), $k_{P1} = 50$ (s^{-2}), $k_{V1} = 1$ (s^{-1}), $k_{FP1} = 1$ (-), $k_{FV1} = 0.01$ (s). In Fig. 10, the results of simulation for the case $k_{c1} = 50$ and selected values of k_{k1} equal to 0 (N/m), 500 (N/m), and 5000 (N/m) respectively is shown. One may notice that along the increase of the value k_{k1} the real trajectory c_{n1} converges with $c_{n1\,nom} + \xi_{01}$ even in the case when the real constraints do not correspond with the theoretical constraints. At the same time the divergence between the desired and the real interaction force increases. It is in a way substituted by a virtual reaction force generated by the second control strategy. On the other hand, the increase of the coefficient k_{c1} results in a decrease of velocity in transients, when a significant divergence of the real constraints from the theoretical constraints occurs. Such a conclusion is a result of analysis of Fig. 11. Fig. 12 shows the influence of amplification k_{k1} when the surface inaccuracy is very significant. For $k_{k1} = 0$, only the force control strategy is applied.

Table 1. Desired trajectory parameters.

Desired trajectory parameters								
param.	v_{max}	w_τ	$F_{e1\,max}$	$c_{\tau 1d}(0)$	t_{c1}	t_{c2}	t_{c3}	t_{c4}
unit	m/s	s^{-1}	N	m	s	s	s	S
value	0,03	5	-10	0,22	2	7	8	8

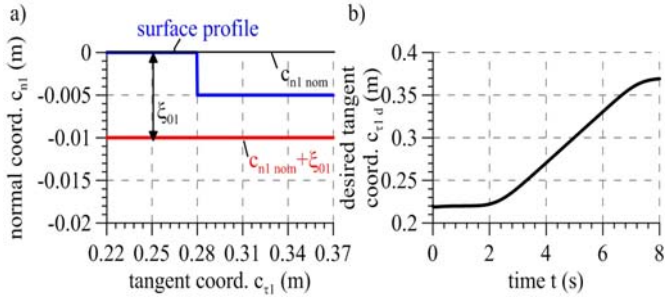

Fig. 9. Desired trajectory of manipulator end-effector: a) nominal path and real constraints (surface profile), b) the desired displacement along the tangential direction.

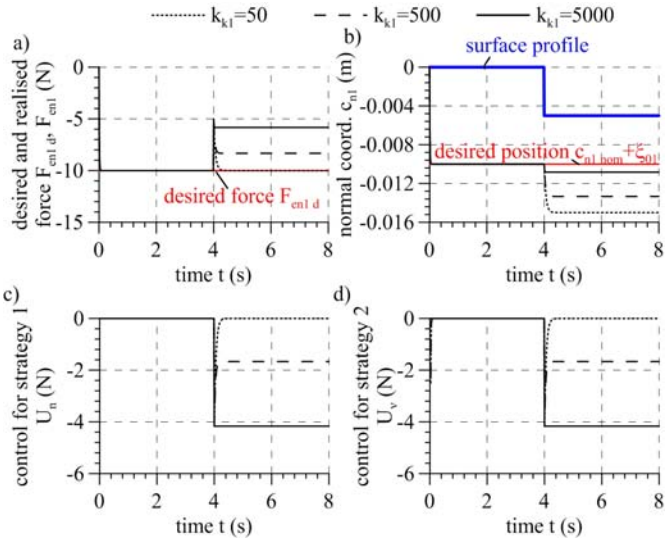

Fig. 10. The results of control strategy implementation for $k_{c1} = 50$ (kg/s) and for different k_{k1} values: a) normal interaction force, b) displacement of manipulator end-effector along the normal direction, c) control signal $U_n = k_{FP1}\tilde{F}_{en1_d} + k_{FV1}\dot{\tilde{F}}_{en1}$ for strategy 1, d) control signal $U_v = k_{k1}\xi_1 + k_{c1}\dot{\xi}_1$ for strategy 2.

In practical applications, it may lead to an impact with a constraint surface. For $k_{k1} > 0$, dislocation on the normal direction is limited despite the lack of a constraint surface. It may be said that the implementation of strategies and the influence of project coefficients in the control system is just as it was assumed at the stage of theoretical analysis.

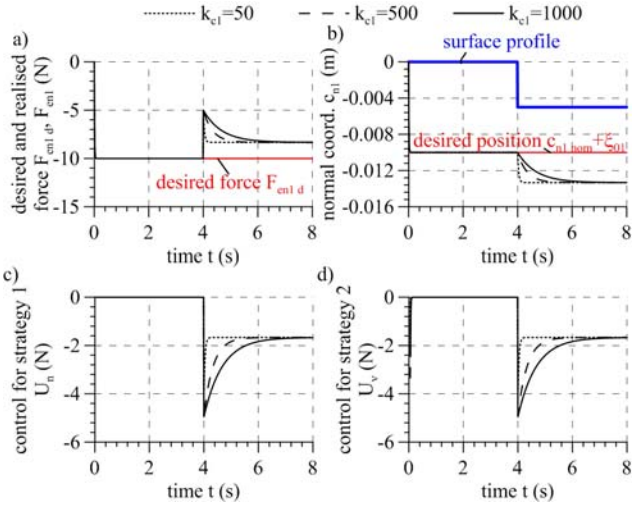

Fig. 11. The results of control strategy implementation for $k_{k1} = 500$ (N/m) and for different k_{c1} values: a) normal interaction force, b) displacement of manipulator end-effector along the normal direction, c) control signal U_n for strategy 1, d) control signal U_v for strategy 2.

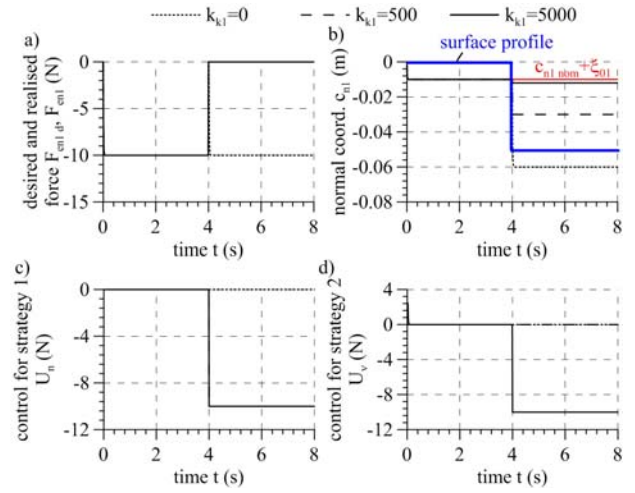

Fig. 12. The results of control strategy implementation for $h_1 = 0.05$ (m) and for different k_{k1} values: a) normal interaction force, b) displacement of manipulator end-effector along the normal direction, c) control signal U_n for strategy 1, d) control signal U_v for strategy 2.

5.2 Results of numerical simulation

This subsection contains results of simulations of differential equations of motion that take the non-linear dynamics of the manipulator into account as per the diagram shown in Fig. 13. The control object parameters are as follows: $a_1 = 0.036$ (kgm^2), $a_2 = 6 \cdot 10^{-5}$ (kgm^2), $a_3 = 0.031$ (kgm^2), $a_4 = 0.54$ (Nms) , $a_5 = 0.51$ (Nms) , $a_6 = 0.05$ (Nm) , $a_7 = 0.025$ (Nm) , $l_1 = 0.22$ (m) , $l_2 = 0.22$ (m) , $\mu = 0.04$ (-). The k_{k1} coefficient value has been selected based on the dependence between error ξ_1 and control amplifications resulting from the solution (61) for the fixed state. Admissible error $\xi_1 = 0.0002$ (m) has been determined, as well as other values of control system. $k_{k1} = 24000$ has been determined. Based on (58), force error will equal $\tilde{F}_{en} = -4.8$ (N). Assuming velocity limit of 0.0033 (m/s), amplification $k_{c1} = 500$ (kg/s) has been determined based on the analysis of solution (61) as well. The issue can be approached differently, i.e. by assuming the force error and determining control amplifications, from which movement parameter errors will result. Fig. 14 shows the results of a numerical simulation and, additionally, courses of analytical solutions of a simplified linear system in order to prove the correctness of assumed simplifications. The control signal in Cartesian space consists of the control based on the mathematical model of the object $u_m = [u_{m1} \quad u_{m2}]^T$ (Fig. 14a) and force control $F_C = [F_{C1} \quad F_{C2}]^T$. The control signal component for the tangential direction $F_{C1} = F_{e\tau}$ is presented in Fig. 14b. The control resulting from the execution of strategies 1 and 2 is shown as well (Fig. 14c and Fig. 14d).

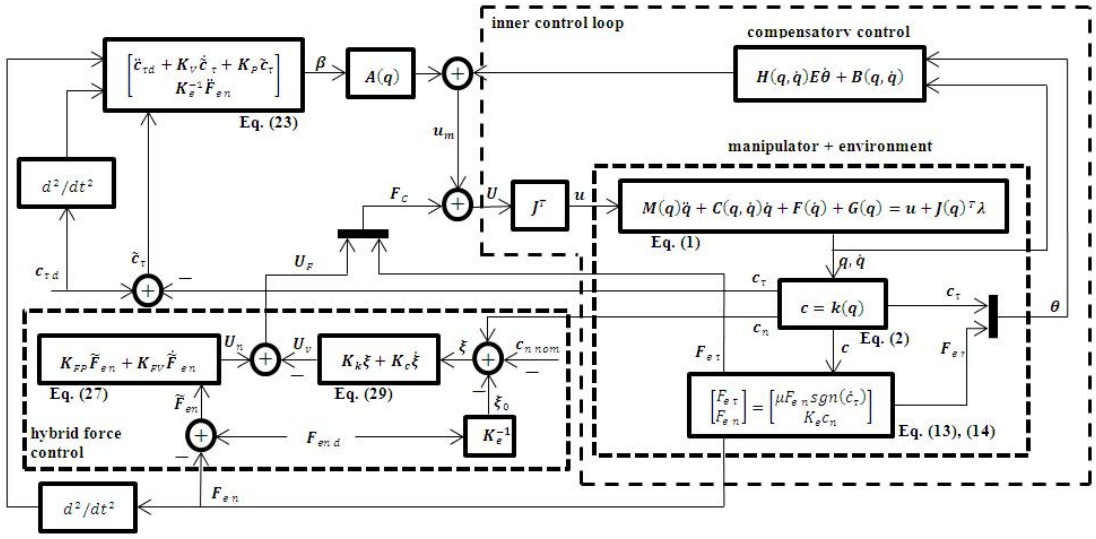

Fig. 13. The scheme of the closed-loop system.

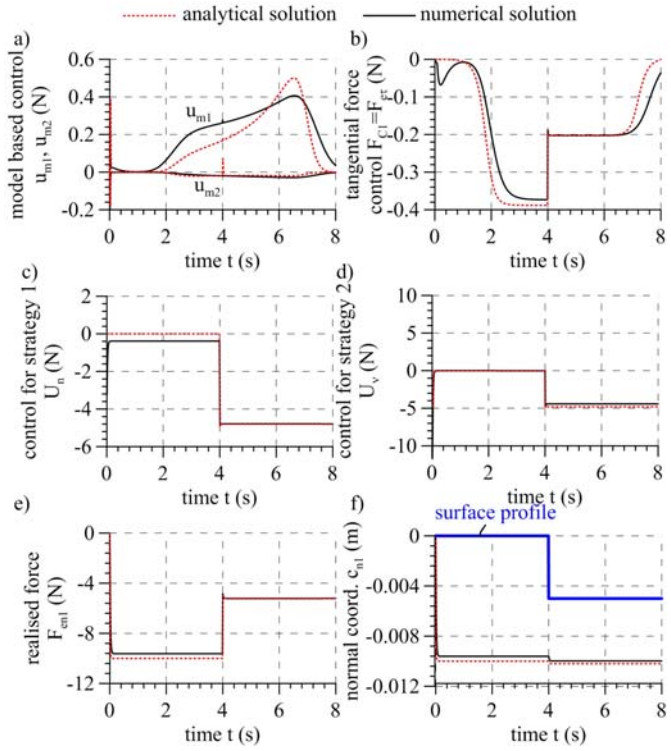

Fig. 14. The results of control strategy implementation: a) control based on the mathematical model of an object $u_m = [u_{m1} \quad u_{m2}]^T = A(q)\beta + H(q,\dot{q})E\dot{\theta} + B(q,\dot{q})$, b) tangential force control – friction compensation, c) control signal U_n for strategy 1, d) control signal U_v for strategy 2, e) normal interaction force, f) displacement of manipulator end-effector along the normal direction.

In the first control phase the strategy 1, responsible for force control, generates the signal U_n approximately at a constant level, whereas the strategy connected with maintaining a constant nominal trajectory in the normal direction in the first stage of motion (until approximately 4 (s), that is, for $c_{\tau 1} \leq 0.28$ (m)) is basically not active – except for the first second of motion, when the manipulator end-effector is pressed against the surface. The strategy 2 is activated in the 4 (s) of motion for $c_{\tau 1} > 0.28$ (m), then the real surface profile changes in relation to the nominal profile of the value $h_1 = 0.005$ (m). The subtraction of controls $U_F = U_n - U_v$ is then stabilized at a certain level, which ensures compromise between the objectives of both strategies. As shown, for $c_\tau > 0.28$ (m), when the manipulator end-effector moves along a cavity (Fig. 14f), the generated clamping force F_{en1} is of a lower value than the desired $F_{en1_d} = 10$ (N), which is a desirable effect in applications connected with machining of such surfaces. It is necessary to notice that all the signals in a closed-loop system remain limited and the system is stable.

6. CONCLUSIONS

The proposed solution introduces a new approach to the implementation of processes in which force control is required and at the same time a significant imprecision or uncertainty of environment description may occur. This method is dedicated for the cases in which the shape of the contact surface is known and its location in relation to the robot is defined. Thanks to appropriate selection of control system parameters, this method ensures insensibility of the system to local defects of the surface such as cavities.

The discussed solution fails to remove all the difficulties occurring in other methods. For example, the necessity of knowing the model of the environment surface still occurs. Additionally, the element β contains the second derivative of the interaction force $\ddot{F}_{en}$ that, in real applications, will be determined based on the measured force signal that includes measurement noise. Such an approach always causes inconvenience. In order to acquire a good-quality signal where differentiation does not "amplify" its high-frequency constituents, filtration methods shall be used, such as those described in (Flixeder et al., 2017).

The scheme of the closed system presented in Fig. 13 contains elements performing the measurement and control, which in real conditions generate delays. However, time constants of mechanical systems such as manipulators are so large, that delays in the measurement and control systems are of no practical significance. At the speed of modern microprocessor systems, the control calculated at 1 kHz and the measurement performed at 10 kHz are standard solutions. Therefore, despite the fact that the measurement and control parts in Fig. 13 are of theoretical nature, only insignificant differences appear in practical implementation because of high mechanical inertia of manipulator.

Nevertheless, the advantage of this solution is that it combines two control strategies in a simple way and they can be implemented simultaneously. Moreover, by selecting the coefficient of control system, a higher priority may be desired to a given strategy.

REFERENCES

Bruhm, H., Czinki, A., and Lotz, M. (2015). High performance force control-A new approach and suggested benchmark tests. *IFAC-PapersOnLine*, *48*(10), 165-170.

Canudas de Wit, C.A., Siciliano, B., and Bastin, G. (1996). *Theory of robot control*. Springer, New York

Capisani, L. M., and Ferrara, A. (2012). Trajectory planning and second-order sliding mode motion/interaction control for robot manipulators in unknown environments. *IEEE Transactions on Industrial Electronics*, 59(8), 3189-3198.

Fanaei, A., and Farrokhi, M. (2006). Robust adaptive neuro-fuzzy controller for hybrid position/force control of robot manipulators in contact with unknown environment. *Journal of Intelligent & Fuzzy Systems*, 17(2), 125-144.

Ferguene, F., and Toumi, R. (2009). Dynamic external force feedback loop control of a robot manipulator using a neural compensator-Application to the trajectory following in an unknown environment. *International Journal of Applied Mathematics and Computer Science*, 19(1), 113-126.

Flixeder, S., Glück, T., Böck, M., and Kugi, A. (2017). Model-Based Signal Processing for the Force Control of Biaxial Gantry Robots. *IFAC-PapersOnLine*, *50*(1), 3208-3214.

Gierlak, P. (2012) Hybrid Position/Force Control of the SCORBOT-ER 4pc Manipulator with Neural

Compensation of Nonlinearities. In: Rutkowski L. et al. (eds) *Artificial Intelligence and Soft Computing. ICAISC 2012. Lecture Notes in Computer Science*, 7268, 433–441. Springer, Berlin, Heidelberg.

Gierlak, P. (2014). Hybrid position/force control in robotised machining. *Solid State Phenomena*, 210, 192-199.

Gierlak, P., and Szuster, M. (2017). Adaptive position/force control for robot manipulator in contact with a flexible environment. *Robotics and Autonomous Systems*, 95, 80-101

Hendzel, Z., Burghardt, A. Gierlak, P., and Szuster, M. (2014). Conventional and fuzzy force control in robotised machining. *Solid State Phenomena*, 210, 178-185.

Lewis, F.L., Abdallah, C.T., and Dawson D.M. (1993). *Control of robot manipulators*. Macmillan, New York.

Lewis, F.L., Jagannathan, S., and Yeşildirek, A. (1999). *Neural network control of robot manipulators and nonlinear systems*. Taylor & Francis, London.

Liu, H., Wang, L., and Wang, F. (2007). Fuzzy force control of constrained robot manipulators based on impedance model in an unknown environment. *Frontiers of Mechanical Engineering in China*, 2(2), 168-174.

Lotz, M., Bruhm, H., and Czinki, A. (2014). An new force control strategy improving the force control capabilities of standard industrial robots. *Journal of Mechanics Engineering and Automation*, 4, 276-283.

Marvel, J., and Falco, J. (2012). Best practices and performance metrics using force control for robotic assembly. US Department of Commerce, National Institute of Standards and Technology.

Pliego-Jiménez, J., and Arteaga-Pérez, M. A. (2015). Adaptive position/force control for robot manipulators in contact with a rigid surface with uncertain parameters. *European Journal of Control*, 22, 1-12.

Tian, F., Lv, C., Li, Z., and Liu, G. (2016). Modeling and control of robotic automatic polishing for curved surfaces. *CIRP Journal of Manufacturing Science and Technology*, 14, 55-64.

Vukobratovič, M., Ekalo, Y., and Rodič, A. (2002). How to apply hybrid position/force control to robots interacting with dynamic environment. In Bianchi, G., Guinot, J.-C., Rzymkowski, C. (ed.), *Romansy* 14, 249-258. Springer, Vienna.

Wu, Y., and Chen, S. (2011). Adaptive neural motion/force control of constrained robot manipulators by position measurement. In *Natural Computation (ICNC), 2011 Seventh International Conference on*, 1, 498-502. IEEE

Xiao, D., Ghosh, B. K., Xi, N., and Tarn, T. J. (2000). Sensor-based hybrid position/force control of a robot manipulator in an uncalibrated environment. *IEEE Transactions on control systems technology*, 8(4), 635-645.

Yu, F., Minami, M., Maeba, T., and Yanou, A. (2011). Constraint-combined force/position hybrid control method with Lyapunov stability. In *SICE Annual Conference (SICE) 2011 Proceedings of*, 671-676. IEEE.

Application manual. Force Control for Machining, ABB Robotics, 2011.